Options for net zero emissions hydrogen from Victorian lignite. Part 1: Gaseous and liquefied hydrogen

## M.A. Kibria [a], D.E. McManus [b,**], S. Bhattacharya [a,*]

[a] Monash University, Department of Chemical and Biological Engineering, PO Box 36, Clayton, Victoria, 3800, Australia
[b] Australian Carbon Innovation, Building 4W-127 Federation University Gippsland, Churchill, Victoria, 3842, Australia

HIGHLIGHTS

- A detailed model for net-zero emissions hydrogen from Victorian lignite proposed.
- Gasification of lignite, production of hydrogen and electricity, with CCS included.
- Fugitive methane emissions during mining included in the model.
- Options exist for greenhouse gas emissions to be consistent with 'Net zero by 2050'.
- Production of low-emissions blue hydrogen from Victorian lignite is feasible.

GRAPHICAL ABSTRACT
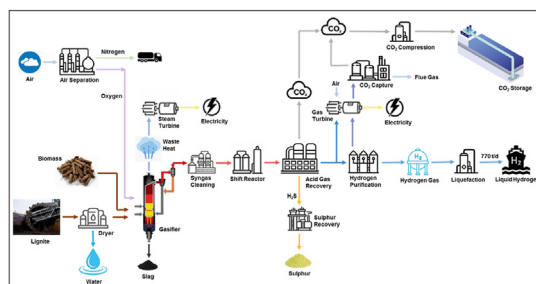
ABSTRACT

This two-part paper investigates the feasibility of producing export quantities (770 t/d) of blue hydrogen meeting international standards, by gasification of Victorian lignite plus carbon capture and storage (CCS). The study involves a detailed Aspen Plus simulation analysis of the entire production process, taking into account fugitive methane emissions during lignite mining. Part 1 focusses on the resources, energy requirements and greenhouse gas emissions associated with production of gaseous and liquefied hydrogen, while Part 2 focusses on production of ammonia as a hydrogen carrier.

In this study, the proposed process comprises lignite mining, lignite drying and milling, air separation unit (ASU), dry-feed entrained flow gasification, gas cooling and cleaning, sour water-gas shift reaction, acid gas removal, pressure swing adsorption (PSA) for hydrogen purification, elemental sulphur recovery, CO_2 compression for transport and injection, hydrogen liquefaction, steam and gas turbines to generate all process power,

* Corresponding author.
** Corresponding author.
E-mail addresses: dmcmanus@acinnovation.com.au (D.E. McManus), sankar.bhattacharya@monash.edu (S. Bhattacharya).

Greenhouse gas intensity
Simulation

plus an optional post-combustion CO_2 capture step. High grade waste heat is utilised for process heat and power generation. Three alternative process scenarios are investigated as options to reduce resource utilisation and greenhouse gas emissions: replacing the gas turbine with renewable energy from off-site wind turbines, and co-gasification of lignite with either biomass or biochar. In each case, the specific net greenhouse gas intensity is estimated and compared to the EU Taxonomy specification for sustainable hydrogen.

This is the first time that a coal-to-hydrogen study has quantified the greenhouse gas emissions across the entire production chain, including upstream fugitive methane emissions. It is found that both gaseous and liquefied hydrogen can be produced from Victorian lignite, along with all necessary electricity, with specific emissions intensity (SEI) of 2.70 kg CO_2-e/kg H_2 and 2.73 kg CO_2-e/kg H_2, respectively. These values conform to the EU Taxonomy limit of 3.0 kg CO_2-e/kg H_2. This result is achieved using a Selexol™ plant for CO_2 capture, operating at 89.5%–91.7% overall capture efficiency. Importantly, the very low fugitive methane emissions associated with Victorian lignite mining is crucial to the low SEI of the process, making this is a critical advantage over the alternative natural gas or black coal processes.

This study shows that there are technical options available to further reduce the SEI to meet tightening emissions targets. An additional post-combustion MDEA CO_2 capture unit can be added to increase the capture efficiency to 99.0%–99.2% and reduce the SEI to 0.3 kg CO_2-e/kg H_2. Emissions intensity can be further reduced by utilising renewable energy rather than co-production of electricity on site. Net zero emissions can then be achieved by co-gasification with ≤1.4 dry wt.% biomass, while a higher proportion of biomass would achieve net-negative emissions. Thus, options exist for production of blue hydrogen from Victorian lignite consistent with a 'net zero by 2050' target.

Nomenclature

Acronyms

CIF	Cost, Insurance and Freight
CCS	Carbon Capture and Sequestration
CO2CRC	Cooperative Research Centre for Greenhouse Gas Technologies
GWP	Global Warming Potential
HESC	Hydrogen Energy Supply Chain
HHV	Higher Heating Value
IGCC	Integrated Gasification Combined Cycle
IPCC	Intergovernmental Committee for Climate Change
LHV	Lower Heating Value
NETL	National Energy Technology Laboratory
PSA	Pressure Swing Adsorption
SEC	Specific Energy Consumption
SMR	Steam Methane Reforming
WTA	*Wirbelschicht Trocknungmitinterner Abwarmenutzung*

Chemicals

CO_2	Carbon dioxide
CO_2-e	Carbon dioxide equivalent
DEPG	Dimethylether polyethylene glycol
H_2	Hydrogen
H_2S	Hydrogen sulphide
MDEA	Methyldiethanolamine
Selexol™	A proprietary blend of DEPG licensed by Honeywell UOP, and the process for its use
TEG	Triethylene glycol

Introduction

To avert the worst impacts of climate change, the scientific consensus is that global temperature rise must be limited to 2 °C above pre-industrial levels, preferably to 1.5 °C. The Paris Agreement specifies that global greenhouse gas emissions should be reduced by 45% by 2030 and reach net zero by 2050 [1]. The Intergovernmental Panel on Climate Change (IPCC) has made it clear that there is a valid role to be played by fossil fuels in 1.5 °C scenarios, provided they are combined with carbon capture and storage (CCS). In its 2014 report, the IPCC highlighted that the cost of stabilizing atmospheric CO_2 would be doubled if the availability of CCS is limited [2]. Meeting the 1.5 °C target will be an enormous challenge, and all available low emissions technologies have a role to play.

Hydrogen will play an important role in reducing CO_2 emissions. There is a range of different clean hydrogen technologies under development, denoted by a spectrum of different colours. The two leading contenders for large-scale deployment are known as blue hydrogen and green hydrogen. Blue hydrogen is produced by fossil fuels with CCS,

mainly through steam methane reforming (SMR) of natural gas or gasification of coal/coke/asphaltenes. Green hydrogen is produced from renewable energy sources, encompassing both gasification of biomass and electrolysis of water using wind or solar power. Currently, blue hydrogen is the lowest cost form of clean hydrogen and is expected to remain so until at least 2030 [3,4].

Blue hydrogen has the advantage that it can leverage many decades of industrial experience in natural gas SMR (e.g. ammonia production), coal gasification, enhanced oil recovery and, to a lesser extent, large scale CCS. There are currently seven commercial facilities producing blue hydrogen by either SMR or gasification [5]. Three demonstration-scale blue hydrogen projects based on SMR have recently been completed [6–8], and another 18 blue hydrogen projects are due for commencement during the 2020s [5].

The actual emissions intensity of blue hydrogen is controversial because of fugitive methane emissions and inefficiencies in CO_2 capture. A recent lifecycle analysis of blue hydrogen from SMR found that the total CO_2-e emissions were only 9%–12% less than for 'grey' hydrogen [9]. However, two subsequent analyses refuted this finding and showed that blue hydrogen can have significantly lower CO_2-e emissions than grey hydrogen, provided that upstream methane emissions are minimised and high CO_2 capture rates are implemented [10,11].

As the international market for clean hydrogen begins to develop, common standards are needed to classify the allowable emissions intensity of different 'colours' of hydrogen. Under the terms of the EU Taxonomy Regulation, the lifecycle greenhouse gas emissions associated with "sustainable" hydrogen must be lower than 3 t CO_2-e/t H_2 [12].

The Climate Bonds Initiative operates a certification scheme for investments consistent with the EU Taxonomy, adopting a "well to gate" approach, which takes account of all upstream lifecycle emissions and all emissions associated with production of hydrogen at 99.9% purity and a gauge pressure of at least 3 MPa [13]. The Climate Bonds Initiative anticipates that the EU Taxonomy limit for hydrogen production will be progressively tightened, reducing to 1.5 t CO_2-e/t H_2 by 2030, then 0.6 t CO_2-e/t H_2 by 2040, with zero carbon emissions by 2050 [13].

Even 100% CO_2 capture during blue hydrogen production cannot compensate for upstream and downstream fugitive emissions, so the only way that the supply chain can be made truly carbon neutral is to incorporate biomass into the production process. Processes combining biomass and CCS allow "neutral" CO_2 to be captured and stored, making it possible to achieve carbon neutral or net negative CO_2-e emissions from blue hydrogen production [14].

In Australia, there is intense interest in production of clean hydrogen for export to Japan, South Korea, and other East Asia markets. However, competition for renewable energy infrastructure to decarbonise the electricity market makes it unlikely that Australia could produce sufficient green hydrogen for export. Blue hydrogen from natural gas and coal feedstocks represents the best opportunity for Australia to contribute to the global clean hydrogen market [15].

The Hydrogen Energy Supply Chain (HESC) Project, supporting Japan's transition to a "hydrogen society", envisages low cost blue hydrogen production by gasification of Victorian lignite with CCS, liquefaction, then transport to Japan by ship [16]. The HESC Project is intended to take advantage of two key resources available in Victoria, Australia. Firstly, the Latrobe Valley contains a potential economic reserve of 33 billion tonnes of lignite, located close to the ground surface and covered with a thin layer of overburden [17]. The lignite typically contains around 60 wt% moisture, restricting its use to near the mine site, so its price is relatively low and not subject to international commodity trading fluctuations.

Secondly, the Latrobe Valley is accessible to at least two high quality CO_2 sequestration sites beneath nearby Bass Strait. The Pelican site, located approximately 8 km off the Gippsland coast and 1.5 km beneath the seabed, has a proven CO_2 storage capacity of at least 125 million tonnes [18]. The depleted Bream oil and gas reservoir, located 46 km offshore, is being redeveloped by ESSO Australia for CO_2 storage, with capacity of up to 1.5 Mt/y to be available to third party users from 2024 [19]. Transportation of CO_2 by pipeline from the Latrobe Valley to sites in Bass Strait is one of the lowest-cost options for CO_2 sequestration in Australia, because of the short transport distance and the high permeability of the storage formations [20].

The practical feasibility of all stages of the HESC concept have been successfully demonstrated. During 2020–2021, the HESC Pilot Project produced hydrogen at 99.999% purity by gasification of Victorian lignite and lignite-biomass blends in the Latrobe Valley. The gaseous hydrogen was transported by road to the Port of Hastings, where it was liquefied and loaded onto the *Suiso Frontier*, the world's first ocean-going liquid hydrogen carrier ship. The *Suiso Frontier* arrived at the Port of Kobe on February 25, 2022 and safely unloaded the hydrogen at a purpose-built receiving terminal and storage facility [21]. Plans to commercialise the HESC concept were announced on March 7, 2023.

In Australia, Victorian lignite is best known as a high-emissions fuel for electricity generation, so it is unclear how it can be used for clean hydrogen production. The purpose of this study is to develop a detailed process simulation model of a plausible lignite-to-hydrogen in Victoria, and to investigate the feasibility of meeting international specifications for blue hydrogen.

A number of process simulation studies have previously been published on hydrogen production via coal gasification with CO_2 capture. Chiesa et al. [22] developed a process concept for hydrogen and electricity co-production based on commercially available technology, involving slurry-fed oxygen-blown, entrained flow coal gasification, sour water–gas shift reactors, Selexol™ acid gas removal, pressure swing adsorption (PSA) for H_2 separation/purification, and gas and steam turbine combined cycles for electricity generation. The H_2S was sent to a sulphur recovery unit comprising an air-blown Claus plant for oxidising H_2S to elemental sulphur, and a SCOT plant for tail gas clean-up. The process delivered purified hydrogen at ~6.2 MPa and compressed CO_2 at 15 MPa pressure, with overall CO_2 capture efficiency of ~95%. The model was constructed using proprietary software and published plant performance data, but the operating conditions were not optimised and the simulation was not calibrated against plant data.

Cormos et al. [23] reported on a ChemCAD simulation to evaluate the performance of an innovative hydrogen production process based on coal gasification with CO_2 capture. The design involved a dry feed gasifier in which CO_2 was used as a coal transport gas, in-plant compression is used to boost the syngas pressure, and 99% (vol.) oxygen purity is used instead of 95% as gasifier oxidant. The process used two sour water-gas shift reactors, Selexol™ acid gas removal, PSA and on-site electricity generation. The process produced 99.99% (vol.) purity H_2 at 6.4 MPa and CO_2 at 11.4 MPa pressure, with overall CO_2 capture efficiency of 93–97% (assumed). In-plant compression of the syngas increased the hydrogen plant output pressure, while hydrogen purity was enhanced by using CO_2 as coal transport gas and by increasing the purity of oxygen used in gasification.

Rath et al. [24] reported a detailed process and cost analysis based on the flowsheet developed by Ref. [23] using state-of-the-art technology available in 2015. An Aspen Plus model was used to estimate stream compositions and assist with equipment sizing, but no details were provided. The plant was designed to produce 25.7 t/h H_2 at 99.9% (vol.) purity and 5.1 MPa pressure by gasification of Illinois #6 coal. CO_2 was captured at 90% efficiency and delivered at a pressure of 15.3 MPa.

Xu et al. [25] developed an Aspen Plus simulation model for a novel coproduction system based on coal partial gasification with CO_2 capture. The process utilised an oxygen-blown, pressurised fluid bed gasifier operating at up to 1000 °C to achieve partial gasification of coal. The syngas was purified using sour water-gas shift catalysts, dry limestone desulphurisation, Selexol™ CO_2 removal (90% efficiency assumed) and PSA. Residual char was combusted in air to raise steam for power generation in a steam turbine. The model was used to investigate the effect of operating conditions on exergy-saving efficiency.

Sevitoglu et al. [26] developed an Aspen Plus simulation model for hydrogen production using a slurry-fed entrained flow gasifier, sour water-gas shift reactors, Selexol™ acid gas removal, PSA, and high temperature electrolyser, with all electricity generated on site using organic Rankine cycle and steam Rankine cycle power units. The system was designed to deliver CO_2 at 15.3 MPa pressure; operating conditions of the PSA unit were not specified. The simulation model was used to assess the likely performance of a range of Turkish low-rank coals (11.6–16.4% moisture content), with Tuncbilek coal (highest C content) achieving the highest overall energy efficiency of 41%.

The above-mentioned references reflect a consensus on the commercial-ready options for syngas processing and hydrogen purification, i.e., CO_2 as a coal transport gas, two-stage water-gas shift reaction, Selexol™ acid gas removal, and PSA. However, none of the proposed schemes are directly applicable to production of liquid hydrogen from Victorian lignite. This is because Victorian lignite contains ~60% moisture, requiring a drying step before dry-feed gasification. Victorian lignite has a low ash content, up to 2% dry matter, and high ash fusion temperature, which are problematic for slag production in downflow entrained flow gasifiers. Also, it is anticipated that, when commercialised, the HESC Project will utilise a dry-feed entrained flow gasifier based on a two-

stage spiral-flow multi-burner design with char recycle [27] currently at 1180 t/d demonstration-scale at the Osaki Cool-Gen Project [28]. Furthermore, previous research on coal-to-hydrogen has not addressed the issues of fugitive methane emissions and overall greenhouse gas intensity.

This study involves detailed simulation modelling of a Victorian lignite-to-hydrogen gasification process with CCS, specifically producing 770 t/d hydrogen from Victorian lignite at 99.999% purity, consistent with the HESC Project concept [16], and in a manner that meets or exceeds the EU Taxonomy specification for sustainable hydrogen. This is the first time that a coal-to-hydrogen study has quantified the greenhouse gas emissions across the entire production chain, including upstream fugitive methane emissions.

The first objective of this study is to develop a detailed simulation of the entire production chain using Aspen Plus V12 simulation software, encompassing lignite mining, lignite drying, entrained flow gasification, hydrogen purification, hydrogen liquefaction and on-site electricity generation, as well as CO_2 capture, compression and pipeline transport for subsurface injection. The second objective is to use the simulation model to investigate alternative processing options to reduce greenhouse gas intensity and resource utilisation, such as utilising off-site renewable power sources and co-gasification with biomass.

System description

The process concept designed to produce blue hydrogen from Victorian lignite is shown in Fig. 1. The process includes all stages from lignite mining through to hydrogen product and CO_2 injection, and accounts for all relevant greenhouse gas emissions including fugitive methane emissions during mining. All water used in the process is derived from the inherent lignite moisture, and most of the necessary electricity is generated from waste heat recovered from the gasifier. Supplementary electricity, if needed, is generated either by burning raw hydrogen and PSA tail gas in a gas turbine, or by off-site wind turbines. The process also includes options for co-gasification of biomass with the lignite, and for supplementary CO_2 removal using a methyldiethanolamine (MDEA) post-combustion scrubber. Purified hydrogen can be produced as either gaseous hydrogen for the domestic market or liquefied for export.

A simulation model of this process was developed using Aspen Plus V12 software. The model implements the process concept of Fig. 1 as a series of high-level Hierarchy blocks, as shown in Fig. 2. The model flowsheet is based on the coal-to-hydrogen process developed by NETL [24], and the Aspen Plus modelling strategy follows the approach originally developed by the Massachusetts Institute of Technology [29] for a NETL coal-to-electricity process [30]. The function of each of the 19 Hierarchy blocks is described in Table 1. Space limitations preclude description of all Hierarchy blocks in this paper, but a full description and specifications are provided in the Supplementary Information. In each Hierarchy block, design and operating conditions are validated against reported industrial data. A summary of the input data and model assumptions is provided in Table 2.
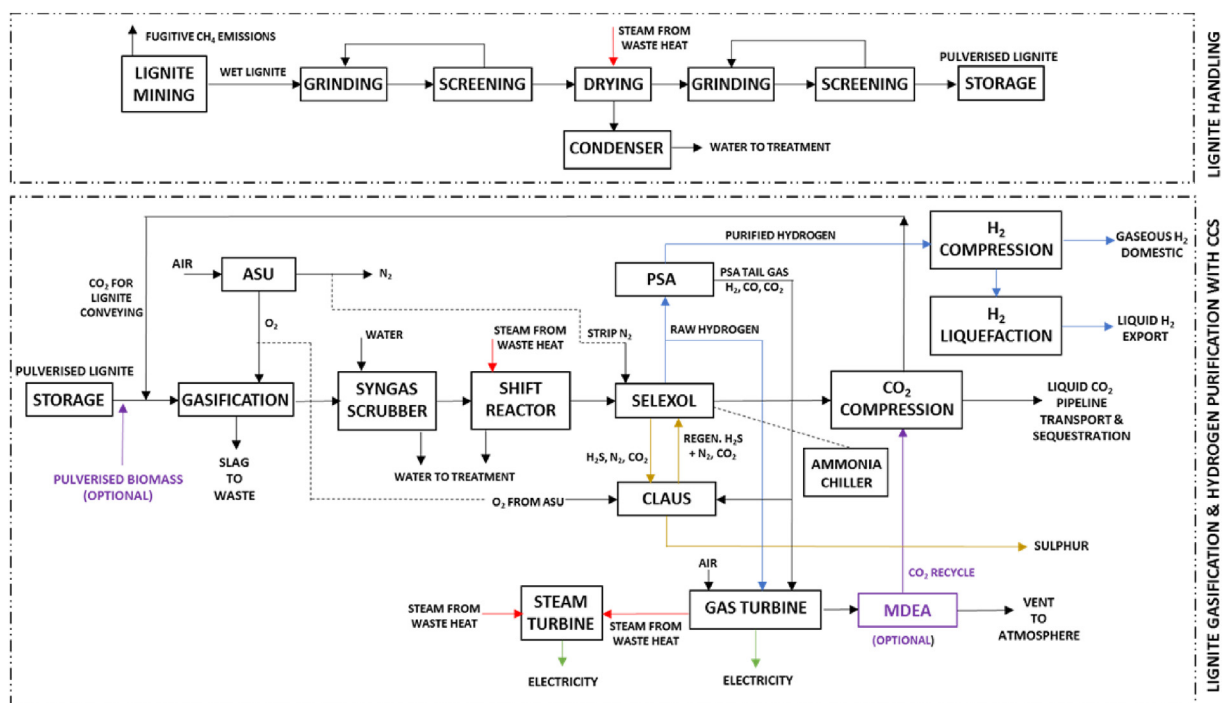
Fig. 1 – Process flow diagram of net zero emission hydrogen from Victorian lignite.
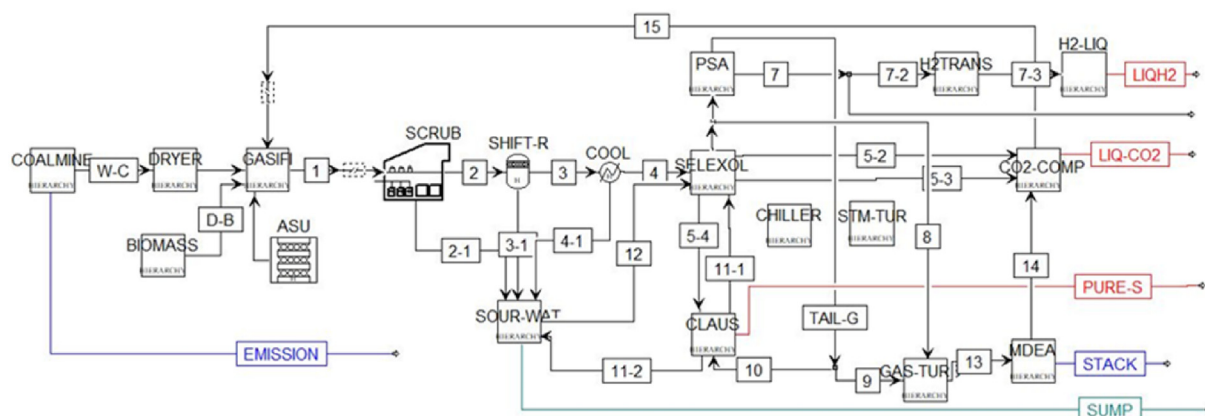

Fig. 2 – High level Aspen Plus process flowsheet for hydrogen production with CCS.

The COALMINE, DRYER, GASIFI, SELEXOL, CLAUS, PSA, H2-LIQ, MDEA and BIOMASS Hierarchy blocks contain aspects that are unique to this process, and are described briefly below.

Lignite mining (COALMINE)

Lignite is extracted at Loy Yang, Victoria using bucket wheel excavators, then loaded onto conveyor belts and transported to storage bunkers. The equipment used in this process is electric-powered, with an average overall energy consumption of 5.17 kW$_e$h/t [31].

The emission factor for fugitive methane emissions from Victorian lignite mining is 0.0162 m^3 CH$_4$/t [32], equating to 11.6 gCH$_4$/t. This is similar to the intensity of fugitive methane emissions reported for German lignite and brown coal mining,

i.e., 0.015 m^3/t [33]. These values are notably lower than those for black coal mining, which range from 3 to 5 m^3/t (50–200 m depth) to 13–18 m^3/t (450–1120 m depth) [34].

Victorian lignite is characterised by low levels of ash, sulphur, heavy metals and nitrogen [35], making it an attractive feedstock for clean hydrogen production. A typical composition of as-mined Loy Yang lignite is shown in Table 3, and was used in the simulation studies.

Lignite drying (DRYER)

The high moisture content of Victorian lignite has long been a barrier to its effective utilisation, so selection of an efficient drying technology is crucial for achieving low cost hydrogen production. Superheated steam drying of lignite has been successfully commercialised in Germany by RWE Power at its

Table 1 − Hierarchy blocks in the lignite-to-hydrogen process.

SI	Hierarchy block	Label	Purpose
1	Lignite mining	COALMINE	Mining of wet lignite
2	Lignite drying, grinding and screening	DRYER	Wet lignite is coarsely pulverised, dried, and then finely pulverised and screened
3	Gasification	GASIFI	Devolatilisation, partial oxidation and gasification of lignite to produce synthesis gas
4	Air separation unit	ASU	Separation of air into O_2 and N_2
5	Gas scrubbing	SCRUB	Removes particulates and impurities by water scrubbing
6	Water gas shift	SHIFT-R	Produces H_2 and CO_2 from CO and steam
7	Syngas cooling	COOL	Reduces the syngas temperature
8	Sour water stripping	SOUR-WAT	Strips out dissolved gases from sour water
9	Acid gas removal	SELEXOL	Separation of H_2S and CO_2 from crude H_2
10	Sulphur recovery	CLAUS	Conversion of H_2S to elemental sulphur
11	Ammonia chiller	CHILLER	Provides cooling for the SELEXOL process
12	Pressure swing adsorption	PSA	Recovery of H_2 to 99.999% purity
13	Hydrogen pipeline	H2-TRANS	Compression and transport of H_2 to liquefaction plant
14	Hydrogen liquefaction	H2-LIQ	Liquefaction of H_2
15	CO_2 compression and transport	CO2-COMP	Compression of CO_2 to supercritical pressure suitable for pipeline transport and injection
16	Gas turbine	GAS-TUR	Generation of electrical power from syngas expansion and by syngas combustion
17	Steam turbine	STM-TUR	Recovery of heat from flue gas and other process heat sources to generate steam used to drive the steam turbines
18	Post-combustion CO_2 capture	MDEA	Captures CO_2 emissions from the gas turbine flue gas
19	Biomass grinding	BIOMASS	Pulverisation and screening of biomass pellets

Niederauβem power station. In this system, known as *Wirbelschicht Trocknungmitinterner Abwarmenutzung* (WTA), or 'fluidised bed drying with internal heat utilisation', the heat of evaporation is recovered by recompressing the vapour to about 0.35 MPa-a and letting it condense inside the fluidised bed heat exchanger tubes [36]. The moisture evaporated from the lignite is thereby recovered for reuse within the process. The WTA plant is normally preceded by two double rotor hammer mills in series, producing raw lignite of ≤2 mm particle size [36]. After drying, an additional grinding unit is needed to reduce the particle size further to meet the specifications of entrained flow gasification.

An Aspen Plus model of the WTA dryer was recently published by our group [37], and is incorporated into the present model. Here, the as-mined lignite is dried from 60% moisture to 10% moisture, while the particle size is reduced from <15 mm to 50−100 μm.

The fluidised bed dryer is simulated using a RStoic reactor, which estimates the amount of energy needed to evaporate the moisture in the lignite and raise it to the bed temperature of 105 °C. The RStoic calculation uses the standard enthalpy of vaporisation of water, assuming that the water can be freely evaporated. However, not all of the water in Victorian lignite behaves like bulk water. A portion of the water is retained by hydrogen bonding in nanopores and stabilised by oxygen groups on exposed surfaces. Below 30% moisture the apparent enthalpy of vaporisation increases steeply, requiring input of extra energy to overcome the binding forces [38]. To compensate for this, an additional dummy heat load with a negative value is added to the model, with a value estimated using a calculator block. Based on experimental data [38], the energy required to dry lignite from 60% to 10% moisture is

estimated to be 0.955 MWh/t dry matter. The calculator block uses this value to adjust the heat load for drying.

Gasification (GASIFI)

The Aspen Plus model of the GASIFI Hierarchy block comprises separate combustion and gasification zones, following the design of the two-stage, spiral-flow gasifier currently under demonstration at the Osaki CoolGen Project [28]. The gasifier is designed to operate at 2.5−3.0 MPa pressure [39]. The lower stage of the reactor is the combustion zone, while gasification occurs in the upper stage. The gasifier section operates below the ash fusion temperature to prevent slag formation and fouling of the walls. Char exiting the gasification zone is recovered from the hot syngas and recycled back to the combustion zone, where the unreacted carbon is burned and the ash minerals melted to slag [27]. This unique configuration allows the combustion zone to be operated at temperatures high enough to create free-flowing slag without requiring fluxing agents. This allows essentially complete carbon conversion at moderate gasification temperatures [39].

Research with Victorian lignite in entrained flow gasification suggests that a gasifier temperature of 1200 °C should achieve a single-pass carbon conversion efficiency of about 95% [40]. The simulation assumes that pulverised lignite is conveyed to the gasifier in a stream of high pressure CO_2, recycled from the downstream CO2-COMP section. It is estimated that CO_2 can convey pulverised lignite effectively using a saltation gas velocity of 6 m/s and a mass flow ratio, CO_2 to dry lignite, of 1.2 kg/kg.

The Aspen Plus model for this two-stage gasifier design was inspired by an AspenTech simulation of the Texaco

Table 2 — Input data and model assumptions.

Lignite mining
　Electrical energy for mining and transport: 5.17 kWh/t
　Fugitive methane emissions: 11.6 g CH_4/t

Lignite drying
　Energy to dry lignite from 60% to 10% moisture: 0.955 MWh/t dry matter.

Air separation unit
　Oxygen purity: 95.0% vol.
　Specific energy consumption: 0.26 kWh/kg

Pneumatic conveying
　Saltation velocity: 6 m/s
　Mass flow ratio of CO_2 to dry lignite: 1.2 kg/kg

Gasification
　Gasifier pressure: 3.2 MPa
　Gasification zone temperature: 1200 °C
　Combustion zone temperature: 1500 °C
　Syngas temperature after Radiant Cooler 1: 600 °C
　Syngas temperature after Radiant Cooler 2: 255 °C

Water-gas shift reactors
　Number of catalytic beds: 2
　CO conversion: 98%
　Steam/CO ratio: 2.0
　Shifted syngas exit temperature: 120 °C

Shifted syngas cooling
　Number of flash coolers: 3
　Cooler exit temperatures F1, F2, F3: 100 °C, 62.5 °C, 39 °C

Acid gas removal system
　Solvent: Selexol™
　CO_2 mole fraction in feed: 0.491
　Selexol™ pressure: 2.9 MPa
　CO_2 capture efficiency: 95.74%
　Mass flow ratio of Selexol™ to CO_2 removed: 19.36 kg/kg
　Electrical duty: 0.012 MW$_e$h/t CO_2
　Reboiler duty: 0.099 MW$_{th}$h/t CO_2

Ammonia chiller
　Generator heat duty: 0.26 kWh/kg of Ammonia before evaporator
　Vapour fraction before evaporator: 0.073
　Cooling load: 0.063 tonne/kg of ammonia

Pressure swing adsorption
　Hydrogen recovery efficiency: 90%
　Hydrogen purity: 99.999% (vol.)
　Energy consumption: 0.5 kWh/kg H_2

Hydrogen liquefaction
　Specific energy consumption: 6 kWh/kg LH_2

Post-combustion CO_2 capture
　Solvent: MDEA
　CO_2 capture efficiency: 90%
　Reboiler duty: 5.39 MJ/kg CO_2 removed

Carbon dioxide compression
　Delivery pressure: 15.3 MPa
　Number of compressor units: 2
　First stage pressure: 1.1 MPa
　Second stage pressure: 8.0 MPa
　Supercritical CO_2 pump efficiency: 75%

Table 3 — Representative composition of Loy Yang lignite.

Moisture (wt.%)	60.0
Proximate analysis (dry, wt.%)	
Volatile matter	42.00
Fixed carbon	55.47
Ash	2.53
Heating value, MJ/kg	
Higher Heating Value	26.00
Lower Heating Value	24.91
Ultimate analysis (dry, wt.%)	
C	68.01
H	4.65
N	0.45
S	0.31
Cl	0.11
Ash	2.53
O	23.94
Ash composition (dry, wt.%)	
SiO_2	56.5
Al_2O_3	20.5
P_2O_5	0.2
Fe_2O_3	4.6
SO_3	5
CaO	1.6
MgO	3.6
K_2O	1.3
Na_2O	4.7

the hot flue gas from the combustion zone. The oxygen and lignite flows are manipulated to achieve a combustion zone temperature of at least 1500 °C, to ensure that ash is fully melted to slag, and a gasification zone temperature of 1200 °C [40].

In both the combustion zone and the gasification zone, the sequence of reactions is modelled using RYield and RGibbs reactors. Lignite pyrolysis is simulated with two RYield reactors. The first RYield reactor is used to simulate lignite pyrolysis at 0.1 MPa based on experimental results obtained in a lab-scale entrained flow reactor operating at 1000 °C [43]. The second RYield reactor is used to adjust the volatile and char yields to 3 MPa conditions using an established correlation [41]. The char is further decomposed to its elemental components in another RYield reactor. Combustion of the evolved volatile matter along with the elemental components obtained from char decomposition is simulated using an RGibbs reactor (RG2 block). The char gasification process is modelled using the RGibbs reactor, which calculates the syngas composition using non-stoichiometric equilibrium modelling.

The energy balance in the combustion zone includes the enthalpy of melting of the ash and the reduction of Fe_2O_3 to Fe and FeO. A reliable method to predict the enthalpy of melting from the ash composition is not available, so the enthalpy was assumed to be the value for aluminium sodium silicate ($NaAlSi_3O_8$), 209.6 kJ/kg [44], which is the major component of the melt (c.f. Table 3). It was assumed that 79.8 wt% of Fe_2O_3 is reduced to Fe and rest is reduced to FeO [29]. The reduction energy is incorporated in the RGibbs reactor (RG2 block) using a calculator block.

Following gasification, two radiant cooling systems are used to cool the hot syngas and recover heat energy for generating steam for power generation in the steam turbine

down-flow entrained flow gasifier [41], as well as our previous work on modelling CO_2 gasification processes [42]. The Aspen Plus model of the GASIFI Hierarchy block is presented in Fig. 3.

In the model, the conveying CO_2 gas and pulverised lignite are mixed together and then split into two streams. One portion, along with oxygen from the air separation unit, enters the combustion zone. Also entering the combustion zone is unreacted char recycled from the syngas. The second portion of lignite/CO_2 enters the gasification zone, where it reacts with
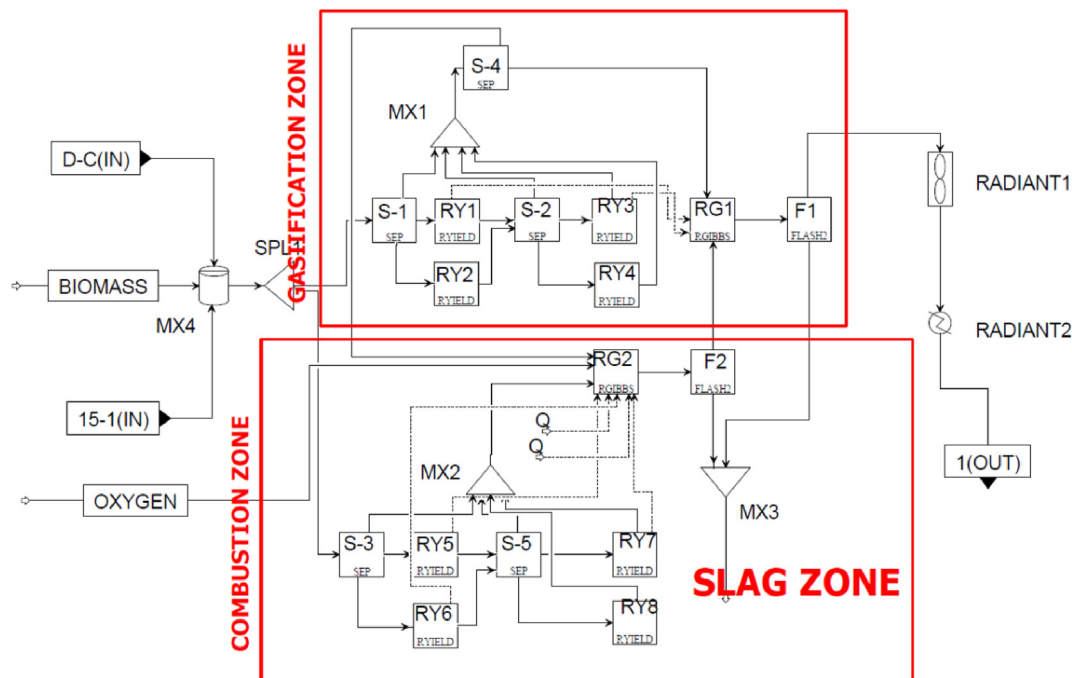
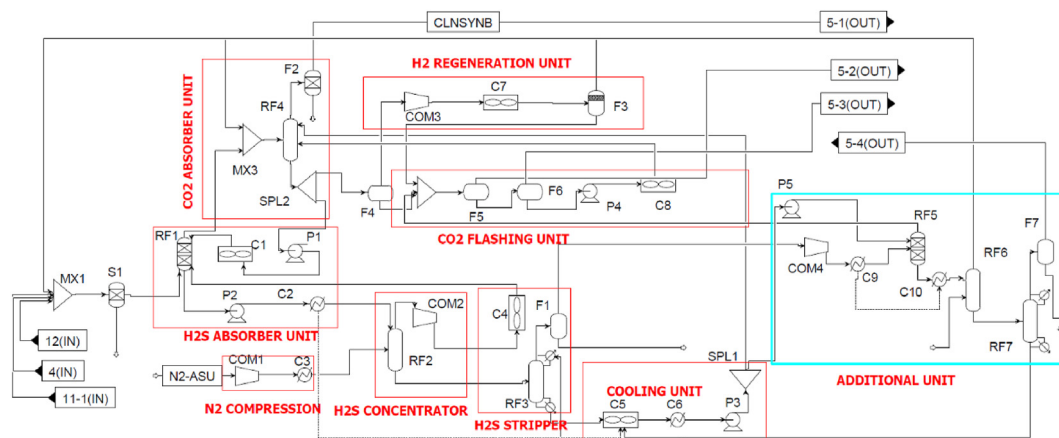Fig. 3 – Aspen Plus model of the GASIFI Hierarchy block.

Fig. 4 – Aspen Plus model of the SELEXOL Hierarchy block.

section. In practice, the syngas cooling section would be followed by an arrangement of cyclones and candle filters to recover unreacted char from the syngas, for recycle back to the combustion zone. In the present case, for the sake of modelling simplicity, char recycle takes place before the radiative coolers. This allows the gasification zone to be conceptually separated from the heat recovery zone, without compromising the accuracy of the simulation results.

Acid gas removal (SELEXOL)

H_2S and CO_2 are removed simultaneously from the shifted syngas using a two-stage Selexol™ process. Selexol™ (DEPG - dimethylether polyethylene glycol) is a 'physical' absorbent, meaning that the solubility of H_2S and CO_2 are dictated primarily by the pressure of the system. The developed Aspen

Plus model for the SELEXOL Hierarchy block, shown in Fig. 4, is based on [22], with two modifications.

The lignite-to-hydrogen process investigated here involved some notable differences to the coal-to-hydrogen study of [29]. Firstly, in Ref. [29] the coal is conveyed as a coal-water slurry into a gasifier pressurised to 5.6 MPa. In the present case, the coal is conveyed pneumatically in a stream of high-pressure CO_2, to a gasifier pressurised to 3.0 MPa. In each case, the pressure of the Selexol™ is synchronised to the gasifier. This means that the mole fraction of CO_2 is higher in the present case, due to the additional conveying CO_2, but there is less driving force for CO_2 removal because of the lower system pressure. Consequently, for the liquid circulation rate specified in Ref. [29], the CO_2 capture efficiency in this case is significantly lower. To compensate, the Selexol™ recirculation rate is increased to boost the mass transfer rate.

Secondly, the sulphur content of Victorian lignite is about nine times less than the black coal considered in Ref. [29], and the difference in solubility between CO_2 and H_2S is less because of the lower system pressure. This causes two problems: an excessive amount of nitrogen is needed to strip CO_2 in the H_2S Concentrator, and the H_2S stream going to the Claus plant is heavily diluted with CO_2, to the point where operation of the Claus plant is compromised. These issues are solved by introducing an additional adsorption/stripping circuit to further concentrate the H_2S stream *en route* to the Claus unit. This is represented by the green block in Fig. 4. A split stream of lean Selexol™ after the main H_2S Stripper is utilised to absorb the additional CO_2.

Sulphur recovery (CLAUS)

The modelling approach used in this study is essentially the same as that described in Ref. [29], with a two-stage modified Claus process used to convert H_2S to elemental sulphur and the sulphur compounds in the tail gas subsequently reduced back to H_2S. In this case, however, rather than incinerating the waste H_2S, it is compressed and recycled to the Selexol™ plant.

Pressure swing adsorption (PSA)

PSA is a dynamic adsorption process that can be readily simulated in Aspen Adsorption but not Aspen Plus. In this study, the PSA unit is modelled using a calculator block, assuming 90% H_2 recovery [45] and an energy consumption of 0.5 kWh/kg H_2 [46].

A portion of the PSA tail gas, containing residual H_2, CO and CO_2, is sent to the CLAUS block, where it is used to reduce unconverted sulphur compounds to H_2S. The PSA tail also contains inert gases, such as nitrogen and argon, which must be purged from the system to prevent accumulation. The purged PSA tail gas is sent to the gas turbine, where it is combusted to produce electricity.

Hydrogen liquefaction (H2-LIQ)

Hydrogen liquefaction can be readily simulated in Aspen HYSYS, but not in Aspen Plus. Linde Kryotechnik AG has developed a cost-optimised design for a 100 t/d hydrogen liquefier with specific energy requirement (SEC) close to or below 6 kWh/kg LH_2 [47]. In the present study, the hydrogen liquefier is modelled using a calculator block, assuming a SEC of 6 kWh/kg LH_2, to simulate the likely performance of next-generation industrial plant.

Post-combustion CO_2 capture (MDEA)

The MDEA block represents a relatively small post-combustion CO_2 scrubbing system on the gas turbine outlet. The Aspen Plus model is based on MDEA solvent and comprises two sections. The first section replicates a rate-based model of MDEA CO_2 capture developed by AspenTech and validated using experimental data [48]. When the flue gas composition after the GT Hierarchy block is substituted into the AspenTech example model, leaving all other parameters unchanged, the example model predicts almost 95% capture efficiency and a reboiler duty of 5.39 MJ/kg CO_2 removed. However, the AspenTech model is specific for equipment with pilot plant dimensions, so the operating conditions and performance cannot be applied to different dimensions.

Accordingly, the second section simulates the MDEA process using a calculator block, with the reboiler duty calculated as 5.39 MJ/kg CO_2 removed, for overall CO_2 capture efficiency of 90%. The reboiler duty is thus based on validated experimental data, while the capture efficiency is conservative.

Biomass grinding (BIOMASS)

Co-gasification with biomass is an acknowledged strategy to achieve carbon neutrality or even net-negative emissions. To investigate this, it is assumed that two types of biomass pellets with contrasting properties are commercially available for use in co-gasification. Based on published composition data of prospective woody waste materials, it is assumed that the pellets available are compressed pine bark and compressed pine bark char. The assumed composition of the pellets is presented in Table 4.

Both types of hypothetical pellets are assumed to be delivered on site at the moisture content shown, and not requiring any additional drying. The greenhouse gas emissions associated with manufacture of the pellets is ignored, due to lack of relevant data.

In the simulation model, a separate grinding and sieving circuit is established to reduce the pellets to a particle size suitable for entrained flow gasification, similar to the lignite. There is limited information available on the energy intensity of biomass grinding. Based on available experimental data, the specific milling energy to mill biomass pellets and biochar pellets to a suitable particle size is assumed to be 327 kWh/t and 34 kWh/t, respectively [49].

Co-gasification of biomass with lignite provides an opportunity to reduce the overall global warming potential (GWP) of blue hydrogen production, as the CO_2 emitted from biomass is carbon neutral. An Excel spreadsheet was constructed to calculate (a) the effect of biomass addition on GWP and (b) the fraction of biomass required for carbon neutrality. Details of the calculations are available in the Supplementary Information.

Space limitations preclude a full description of the modelling approach in this paper but all details, including

Table 4 – Composition of pine bark and pine bark char.		
Component	Pine bark [50]	Pine bark char [51]
Proximate analysis (as received, wt%)		
Moisture	7.72	2.31
Volatile matter	69.30	20.24
Fixed carbon	20.84	61.70
Ash	2.14	15.75
HHV (MJ/kg)	20.10	25.30
LHV (MJ/kg)	18.98	24.73
Ultimate analysis (dry, wt%)		
C	48.90	69.86
H	4.95	2.57
N	0.21	0.35
S	0.18	0.04
Ash	2.14	15.75
O	43.62	11.43

Table 5 — Summary of simulation modelling results.

Process inputs	GH2	LH2	LH2-R	LH2-BM	LH2-BC
As-mined lignite feed rate, t/h	820	1050	800	902	825
Pulverised lignite feed rate, t/h	364.4	466.7	355.6	400.9	366.7
Biomass/char feed rate, t/h	0	0	0	98	84.5
Oxygen flowrate, t/h	270	345	263	336	328
Process outputs					
Purified H_2 production, t/h	32.4	32.4	32.4	32.4	32.4
Sulphur production, t/h	0.9	1.1	0.9	1.1	0.9
Water from lignite dryer, t/h	456	584	444	501	459
Slag production, t/h	8.2	10.8	8.2	11.4	21.8
CO_2 sequestered (no MDEA), t/h	835.3	1170.9	816.0	1093.2	1055.7
CO_2 to atm. (no MDEA), t/h	86.4	87.4	68.4	92.3	89.5
CO_2 sequestered (MDEA), t/h	834.4	1249.6	877.6	1176.3	1136.2
CO_2 to atm. (with MDEA), t/h	8.6	8.7	6.8	9.2	8.9
Fugitive methane emissions, t/h	0.010	0.012	0.009	0.010	0.010
Electrical power					
Total power required, MW_e	240	481	412	502	465
Total power generated, MW_e	265	481	155	502	466
Excess capacity, MW_e	25	0	−257	0	1
Thermal power					
Thermal power required, MW_{th}	977	1171	891	1202	1177
Thermal power recovered, MW_{th}	978	1174	909	1218	1193
Actual capture efficiency of Selexol™ plant					
Capture efficiency, %	92.3	93.8	93.6	93.7	93.7
Apparent capture efficiency of CO_2 in syngas, %					
Selexol™ only	89.5	91.7	91.4	91.4	91.4
Selexol™ plus MDEA	99.0	99.2	99.2	99.1	99.1
% Biomass for CO_2-e neutrality					
Selexol™ only	14.1	11.2	11.6	—	—
Selexol™ plus MDEA	1.4	1.2	1.2	—	—

heat integration and greenhouse emissions calculations, can be found in the Supplementary Information.

Results and discussion

The process simulation model was used to investigate the feasibility of blue hydrogen production from Victorian lignite in five different scenarios. In each case, the hydrogen production rate was fixed at 32.4 t/h, i.e. ~770 t/d, consistent with the original HESC Project concept [16].

(1) GH2: Production of gaseous hydrogen for the domestic market, generating all necessary electrical power on site using a combination of a waste heat steam turbine and a gas turbine.

(2) LH2: Production of liquefied hydrogen for export, generating all necessary electrical power on site.

(1) LH2-R: Production of liquefied hydrogen from lignite, generating electrical power on site using a waste heat steam turbine and sourcing additional electricity from external renewable sources. This is similar to the original HESC Project scenario.

(2) LH2-BM: Production of liquefied hydrogen by co-gasification of 20% biomass (dry basis) with lignite, generating all necessary electrical power on site.

(3) LH2-BC: Production of liquefied hydrogen by co-gasification of 20% biochar (dry basis) with lignite, generating all necessary electrical power on site.

The results of the modelling for each scenario are summarised in Table 5, with the detailed results available in the Supplementary Information.

Lignite gasification

LH2-R has the lowest lignite consumption rate, equating to 7.0 Mt/y. About 30 Mt/y lignite is currently mined at Loy Yang, so LH2-R represents about 23% of current lignite consumption. However, this scenario has a net deficiency of 257 MW electrical power, which must be supplied by renewable energy sources.

LH2 has the highest lignite consumption rate, equating to 9.2 Mt/y, which is about 30% of the rate currently mined at Loy Yang. However, this allows the plant to be self-sufficient for electricity production and not dependent on external sources.

The lignite requirement in GH2 is only slightly higher than that in LH2-R, equating to 7.2 Mt/y, because it does not include liquefaction of hydrogen, a large energy consumer.

Electrical power consumption

Of the three lignite-only scenarios, GH2 had the lowest electrical power consumption, at 240 MWe. In this case, gasification of lignite to produce 32.4 t/h H_2 produced enough waste heat energy to generate all the electricity needed for the process plus an excess of 25 MW which could be sold to the grid.

The energy consumption in LH2 was double that in GH2, at 481 Mwe. Due to the high energy intensity of H_2 liquefaction
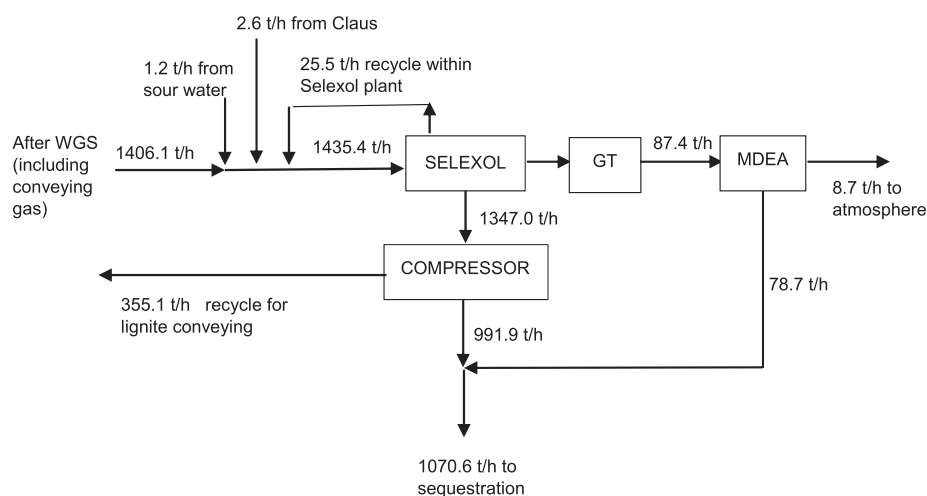
Fig. 5 – CO$_2$ flowrates relevant to Selexol™ plant efficiency in LH2.

(176 MWe), it was necessary to gasify additional lignite and divert some of the crude hydrogen product to the gas turbine to generate more electricity. This required larger gasification and gas treatment plant capacity, further increasing the electricity demand.

In LH2-R, the electrical energy consumption was somewhat lower than in LH2, at 412 MWe. In this case, the only electricity generated on-site was 155 MWe from waste heat via the steam turbine, with 257 MWe sourced externally from renewable energy providers.

Surprisingly, LH2-BM had the highest electricity consumption, at 502 Mwe, because of the high energy penalty (32 MW) associated with fine grinding of the biomass. LH2-BC had a slightly lower electricity requirement (465 MWe) than LH2, because the is easier to grind than biomass and displaces some of the energy load associated with lignite drying.

Co-gasification of lignite with biomass and biochar

LH2-BM and LH2-BC are variations on LH2, where 20% of the feedstock dry mass is substituted by biomass pellets and biochar pellets, respectively (compositions shown in Table 4). From a gasification perspective, the performance of biochar is very close to that of lignite, because they have very similar fixed carbon contents and higher heating values. Consequently, similar amounts of CO$_2$ and waste heat are produced.

In contrast, biomass contains less fixed carbon and lower heating capacity, so less CO$_2$ and waste heat are produced. Less CO$_2$ production reduces the load on the Selexol™, chiller and MDEA units, but this is more than offset by the increased energy requirement for biomass grinding.

CO$_2$ capture efficiency

The model includes two options for CO$_2$ emission control. The vast majority of the CO$_2$ is captured in the Selexol™ plant, which is a core and essential part of the process. A post-combustion 'polishing' CO$_2$ capture step, using activated MDEA, is positioned after the gas turbine as an optional feature that can be deployed in response to tightening emissions specifications for blue hydrogen.

The studied process involves a number of internal recycle loops which return spent streams containing SO$_2$ and CO$_2$ to the Selexol™ unit for reprocessing. These must all be accounted for in determining the capture efficiency of the Selexol™ process. As an example, Fig. 5 shows the CO$_2$ flows relevant to estimating the capture efficiency for the LH2 scenario.

The CO$_2$ capture efficiency of the process can be expressed in two ways. The 'actual' capture efficiency of the Selexol™ plant is based on the sum of CO$_2$ mass flows at the inlet and outlet of the unit. In the example shown, the actual capture efficiency is 1347.0/1435.4 = 93.8%. The 'actual' efficiency takes into account the extra load associated with recycle streams of CO$_2$ within the process.

The 'apparent' capture efficiency is the overall efficiency of capturing and sequestering the CO$_2$ generated from the feedstock in the water-gas shift reactor, excluding the CO$_2$ used as conveying gas. In the example shown, the CO$_2$ directly attributable to the feedstock is 1406.1−355.1 = 1051.0 t/h. The amount of CO$_2$ captured for sequestration is affected by the presence of recycle streams within the plant, so the CO$_2$ released to atmosphere provides the most straightforward measure of capture efficiency. In this case, the apparent capture efficiency is 1 − (July 8, 1051.0) = 99.2%. Without the MDEA unit, the apparent capture efficiency is 91.7%.

Under the selected operating conditions, the actual capture efficiency of the Selexol™ plant was estimated to range from 92.3% to 93.8% over the 5 scenarios. With only the Selexol™ plant operational, the apparent CO$_2$ capture efficiency ranged from 89.5% to 91.7%. Adding the post-combustion MDEA unit increased the capture efficiency to 99.0–99.2%.

It would not be economical to reduce the emissions intensity further by trying to boost the efficiency of the Selexol™ and MDEA units, as the increased power requirement would be counterproductive. Nor would the fugitive methane emissions associated with lignite mining be mitigated by increasing the capture efficiency.

An alternative strategy to offset the remaining emissions and achieve carbon neutrality is to co-gasify biomass along with the lignite. CO$_2$ from biomass is carbon neutral when released, and carbon negative when permanently sequestered.

Table 6 — Assignment of Global Warming Potential values to CO_2 mass flows.

Assigned GWP, t CO_2-e/h	GH2	LH2	LH2-R	LH2-BM	LH2-BC
a) Selexol™ only					
Lignite mining	0.3	0.3	0.3	0.3	0.3
Captured lignite CO_2	0	0	0	0	0
Captured biomass CO_2	–	–	–	−137.6	−196.5
Released lignite CO_2	86.4	87.4	68.4	72.0	72.0
Released biomass CO_2	–	–	–	0	0
Total GWP	**86.7**	**87.7**	**68.7**	**−65.3**	**−124.3**
b) Selexol™ plus MDEA					
Lignite mining	0.3	0.3	0.3	0.3	0.3
Captured lignite CO_2	0	0	0	0	0
Captured biomass CO_2	–	–	–	−149.2	−213.1
Released lignite CO_2	8.6	8.7	6.8	7.5	7.5
Released biomass CO_2	–	–	–	0	0
Total GWP	**8.9**	**9.0**	**7.1**	**−141.4**	**−205.3**

Bold indicates the key number or key information.

Using the Selexol™ plant alone for CO_2 capture, the proportion of biomass required for carbon neutrality is 14.1%, 11.9% and 11.6% for scenarios GH2, LH2 and LH2-R, respectively. This equates to biomass consumption rates of 438 kt/y, 448 kt/y and 353 kt/y, respectively. It would be a significant challenge to source such quantities of biomass from Victorian forests.

With the MDEA unit operational, the proportion of biomass required falls to 1.4 dwt%, 1.2 dwt% and 1.2% for scenarios GH2, LH2 and LH2-R, respectively. This equates to biomass feeding rates of 44.7 kt/y, 45.5 kt/y and 35.0 kt/y, respectively. These quantities of biomass could potentially be sourced in Victoria from recycled timber waste.

Net global warming potential

The global warming potential (GWP) of each scenario is shown in Table 6. For LH2, GH2 and LH2-R, the total GWP equates to the total flow of CO_2 escaping the capture system, plus the contribution from fugitive methane emissions during mining. LH2-R, with MDEA operational, has the lowest GWP of the three because extra lignite is not consumed for power generation.

LH2-BM and LH2-BC involve substitution of 20% of the feedstock dry mass with biomass pellets and biochar pellets, respectively. The quantities involved are likely to be unrealistic, but these scenarios are mainly intended to highlight the potential of co-gasification, which is to achieve net-negative GWP. From these results, biochar appears to have greater potential for net-negative emissions than biomass. However, this analysis does not take into account the CO_2 emissions generated during the production of biochar, so a full life cycle analysis is required to assess the relative merits of biochar versus biomass.

Specific CO_2 emissions intensity

The data from Table 6 can be used to calculate the specific CO_2-e emissions intensity (SEI) for production of 32.4 t/h H_2, as shown in Table 7. The EU Taxonomy specification is standardised for a hydrogen pressure of 3 MPa gauge, whereas in this model the purified hydrogen exits the PSA at 27.5 bar (2.65 MPa gauge). Separate modelling (results not shown) indicated that boosting the exit pressure to 3 MPa gauge would require 8.8 MW extra electricity and would create 0.8 t/h of additional CO_2 emissions. Table 7 presents the SEI results for each scenario, adjusted to the specified EU Taxonomy conditions.

The results of this analysis show that, for each of the scenarios studied, the SEI of blue hydrogen from Victorian lignite can meet the EU Taxonomy specification. Under current specifications, gaseous and liquefied hydrogen can both be co-produced, along with all necessary electricity, using only the Selexol™ plant for CO_2 capture, with SEI of 2.7 kg CO_2-e/kg H_2 and 2.73 kg CO_2-e/kg H_2, respectively. The SEI can be reduced further by using renewable energy rather than co-generation, and by co-firing with biomass or biochar.

This unexpected result can largely be attributed to the very low level of methane emissions released during mining of Victorian lignite, with an emission factor of only 0.0162 m^3/t mined [32]. For LH2, the specific rate of fugitive methane emissions amounts to 0.011 kg CO_2-e/kg H_2, while for LH2-R it is 0.006 kg CO_2-e/kg H_2.

The EU Taxonomy specification will be progressively lowered to meet a target of net zero by 2050, with anticipated limits of 1.5 t CO_2-e/t H_2 by 2030 and 0.6 t CO_2-e/t H_2 by 2040 [13]. The results in Table 7 show that these specifications can readily be achieved by installing a post-combustion MDEA CO_2 capture plant after the gas turbine, thereby reducing the SEI to a maximum of 0.3 kg CO_2-e/kg H_2. With this unit in place, net zero emissions could be achieved by co-gasification with ≤1.4 dry wt.% biomass. Co-gasification with a higher proportion of biomass would result in net-negative emissions intensity,

Table 7 — Specific CO_2 emission intensity for blue hydrogen production.

Assigned GWP, t CO_2-e/h	GH2	LH2	LH2-R	LH2-BM	LH2-BC
Selexol™ only	86.7	87.7	68.7	−65.3	−124.3
Selexol™ plus MDEA	8.9	9.0	7.1	−141.4	−205.3
Additional emissions to boost pressure from 27.5 bar to 31 bar (according to EU Taxonomy)					
Extra emissions, t CO_2-e/h	0.8	0.8	0.8	0.8	0.8
Adjusted GWP, t CO_2-e/h					
Selexol™ only	87.5	88.5	69.5	−64.5	−123.5
Selexol™ plus MDEA	9.8	9.8	7.9	−140.6	−204.5
Specific emission intensity, kg CO_2-e/kg H_2 @ 3 MPa gauge pressure					
Selexol™ only	2.70	2.73	2.14	−1.99	−3.81
Selexol™ plus MDEA	0.30	0.30	0.24	−4.34	−6.31

Table 8 – Net water balance for each scenario.					
	GH2	LH2	LH2-R	LH2-BM	LH2-BC
Water from lignite dryer, t/h	456	584	444	501	459
Water used in shift reactor, t/h	−363	−464	−354	−482	−489
Condenser & cooling tower, t/h	−1035	−1325	−1009	−1376	−1350
Water to trade waste, t/h	−46	−64	−33	−51	−51
Totals	−988	−1269	−952	−1408	−1431

dependent on the availability of sustainable quantities of biomass.

Water consumption

This study included a preliminary analysis of water consumption in the lignite-to-hydrogen process, as shown in Table 8. Victorian lignite is a potentially valuable source of water that can be recovered for reuse in the process. However, a detailed analysis of water consumption in the process was not possible because of the high degree of uncertainty about water consumption during waste heat recovery. It is known that steam turbine condensers and cooling towers are net consumers of environmental make-up water, but there is little guidance available in the public literature to estimate the quantities involved. The only findable reference on water losses associated with steam turbines and cooling towers is the NETL coal-to-hydrogen study [24], from which a scaling factor of 1.86 t makeup water/t CO in syngas was derived. A preliminary estimate was also made of the potential losses of water to trade waste from the wastewater treatment system (see the Supplementary Information for details). The resulting water balance is shown in Table 8.

This analysis shows that drying lignite from 60% to 10% moisture in the WTA dryer produces enough water for hydrogen production in the shift reactor, significantly reducing the environmental impact. However, the overall water balance is dominated by the high evaporative losses during waste heat recovery. As a result, each of the scenarios considered is a net water consumer. For example, LH2 is estimated to require 1269 t/h make-up water, equating to around 11 GL/year.

It is anticipated that this water requirement could be significantly reduced using a more efficient heat recovery scheme. This will be addressed in a subsequent study.

Conclusion and limitations

This study involves development of a process model in Aspen Plus to examine the potential benefits of producing gaseous and liquified blue hydrogen from Victorian lignite in Australia. This study presents an innovative approach for the production of hydrogen using the water found in Victorian lignite, rather than depending on other environmental resources for water, which is particularly relevant for Australia. It is shown that both gaseous and liquefied hydrogen can be produced from Victorian lignite, co-generating all required electricity

on-site, with emissions intensity less than the EU Taxonomy limit for sustainable hydrogen. The emissions intensity can be reduced further by sourcing renewable energy off-site and by implementing an optional post-combustion CO_2 capture unit. After that, net zero emissions could be achieved by co-gasification with ≤1.4 dry wt.% biomass. Co-gasification with a higher proportion of biomass would achieve net-negative emissions.

This study demonstrates the feasibility of producing blue hydrogen from Victorian lignite consistent with a 'net zero by 2050' target. Production of blue hydrogen in Victoria has four distinct competitive advantages over other modes of production: (i) an effectively inexhaustible supply of low-cost feedstock, (ii) very low levels of fugitive methane emissions during mining, (iii) an inherent supply of water that can be utilised for hydrogen production, and (iv) proximity to massive, high quality CO_2 storage reservoirs. This study supports the development of blue hydrogen from Victorian lignite as a new export industry for Australia.

Further research is recommended to address some limitations of this preliminary study. While the greenhouse gas emissions associated with lignite mining were accounted for in this study, a lack of relevant data meant that the emissions associated with production and transport of biomass and biochar pellets were not included. No published studies were found to establish the feasibility of a biomass pellet industry in Australia, so further work in this area is required.

Another limitation of this study is that it looked only at recovery of high-grade waste heat, but did not consider options for utilisation of low-grade waste heat. This would require a more detailed heat integration analysis, beyond the capability of the current process model. However, this is an essential next step for estimation of the water losses in the steam turbine condenser and cooling towers.

Similarly, a lack of relevant information on the wastewater treatment steps likely to be required meant that this could not be included in the simulation model. Experimental research is required on the treatment and reuse options for the WTA condensate water, to support a more detailed engineering study.

In view of the competing views about whether liquid hydrogen or ammonia is the better option as a hydrogen carrier, Part 2 of this study will extend the process simulation model to the production of low emissions ammonia from Victorian lignite. This will allow the relative merits of both options to be investigated on an equivalent basis.

Declaration of Competing Interest

The authors declare that they have no known competing financial interests or personal relationships that could have appeared to influence the work reported in this paper.

Acknowledgements

based company, with the support of the Victorian Government.

Appendix A. Supplementary data

Supplementary data to this article can be found online at https://doi.org/10.1016/j.ijhydene.2023.04.213.

REFERENCES

[1] United Nations environment program Addendum to the Emissions Gap Report 2021. p. 1–6. https://wedocs.unep.org/bitstream/handle/20.500.11822/37350/AddEGR21.pdf [Accessed 8 December 2022].

[2] Pachauri R, Meyer L. Climate change 2014: synthesis report. Contribution of working groups I, II and III to the fifth assessment report of the intergovernmental Panel on climate change. 2014. https://www.ipcc.ch/report/ar5/syr. [Accessed 8 December 2022].

[3] International energy agency. The future of hydrogen. https://www.iea.org/reports/the-future-of-hydrogen. [Accessed 8 December 2022].

[4] Ahmed SF, Mofijur M, Nuzhat S, Rafa N, Musharrat A, Lam SS, et al. Sustainable hydrogen production: technological advancements and economic analysis. Int J Hydrogen Energy 2022;47:37227–55. https://doi.org/10.1016/j.ijhydene.2021.12.029.

[5] Global CCS Institute. Blue hydrogen. https://www.globalccsinstitute.com/resources/publications-reports-research/blue-hydrogen. [Accessed 8 December 2022].

[6] Preston C. The carbon capture project at Air Products' Port Arthur hydrogen production facility. 14th Greenhouse Gas Control Technologies Conference Melbourne 21-26 October 2018 (GHGT-14); 1:1-4 https://doi.org/10.2139/ssrn.3365795.

[7] Stantec Consulting. Quest carbon capture and storage project. Calgary, Alberta: Project description. Stantec Consulting Inc.; 2010. https://open.alberta.ca/dataset/7fc3495c-4659-4712-9ee4-8fe7e39f03b8/resource/bae2d1e1-d2e6-4e0f-a779-c05912254bdb/download/01-quest-vol-1-project-description.pdf. [Accessed 8 December 2022].

[8] Tanaka Y, Sawada Y, Tanase D, Tanaka J, Shiomi S, Kasukawa T. Tomakomai CCS demonstration project of Japan, CO_2 injection in process. Energy Proc 2017;114:5836–46. https://doi.org/10.1016/j.egypro.2017.03.1721.

[9] Howarth RW, Jacobson MZ. How green is blue hydrogen? Energy Sci Eng 2021;9:1676–87. https://doi.org/10.1002/ese3.956.

[10] Bauer C, Treyer K, Antonini C, Bergerson J, Gazzani M, Gencer E, et al. On the climate impacts of blue hydrogen production. Sustain Energy Fuels 2022;6:66–75. https://doi.org/10.1039/D1SE01508G.

[11] Romano MC, Antonini C, Bardow A, Bertsch V, Brandon NP, Brouwer J, et al. Comment on "How green is blue hydrogen?". Energy Sci Eng 2022. https://doi.org/10.1002/ese3.1126.

[12] EU Taxonomy Compass. Manufacture of hydrogen. https://ec.europa.eu/sustainable-finance-taxonomy/activities/activity/155/view. [Accessed 8 December 2022].

[13] Dillman K, Heinonen J. A 'Safe' Hydrogen Economy: An Absolute Environmental Sustainability Assessment of the Hydrogen Economy, 1:1–29. https://doi.org/10.2139/ssrn.4081110.

[14] Hetland J, Yowargana P, Leduc S, Kraxner F. Carbon-negative emissions: systemic impacts of biomass conversion: a case study on CO_2 capture and storage options. Int J Greenh Gas Control 2016;49:330–42. https://doi.org/10.1016/j.ijggc.2016.03.017.

[15] Boretti A. Production of hydrogen for export from wind and solar energy, natural gas, and coal in Australia. Int J Hydrogen Energy 2020;45:3899–904. https://doi.org/10.1016/j.ijhydene.2019.12.080.

[16] Kamiya S, Nishimura M, Harada E. Study on introduction of CO_2 free energy to Japan with liquid hydrogen. Phys Procedia 2015;67:11–9. https://doi.org/10.1016/j.phpro.2015.06.004.

[17] Holdgate GR, McGowran B, Fromhold T, Wagstaff BE, Gallagher SJ, Wallace MW, et al. Eocene–Miocene carbon-isotope and floral record from brown coal seams in the Gippsland Basin of southeast Australia. Global Planet Change 2009;65:89–103. https://doi.org/10.1016/j.gloplacha.2008.11.001.

[18] Earth resources. The CarbonNet project. State government of Victoria. https://earthresources.vic.gov.au/projects/carbonnet-project. [Accessed 8 December 2022].

[19] The South East Australia carbon capture hub. https://www.exxonmobil.com.au/energy-and-environment/energy-resources/upstream-operations/the-south-east-australia-carbon-capture-hub. [Accessed 8 December 2022].

[20] CO2CRC. Australian power generation technology report. http://earthsci.org/mineral/energy/coal/LCOE_Report_final_web.pdf. [Accessed 8 December 2022].

[21] HESC. Successful completion of pilot project report. https://www.hydrogenenergysupplychain.com/report-successful-completion-of-the-hesc-pilot-project. [Accessed 8 December 2022].

[22] Chiesa P, Consonni S, Kreutz T, Williams R. Co-production of hydrogen, electricity and CO2 from coal with commercially ready technology. Part A: performance and emissions. Int J Hydrogen Energy 2005;30:747–67. https://doi.org/10.1016/j.ijhydene.2004.08.002.

[23] Cormos C-C, Starr F, Tzimas E, Peteves S. Innovative concepts for hydrogen production processes based on coal gasification with CO_2 capture. Int J Hydrogen Energy 2008;33:1286–94. https://doi.org/10.1016/j.ijhydene.2007.12.048.

[24] Rath LK, Chou VH, Kuehn NJ. Assessment of hydrogen production with CO_2 capture volume 1: baseline state-of-the-art plants. Pittsburgh, PA, Morgantown, WV: National Energy Technology Laboratory (NETL); 2011. https://www.osti.gov/servlets/purl/1767148. [Accessed 8 December 2022].

[25] Xu Y, Zang G, Chen H, Dou B, Tan C. Co-production system of hydrogen and electricity based on coal partial gasification with CO_2 capture. Int J Hydrogen Energy 2012;37:11805–14. https://doi.org/10.1016/j.ijhydene.2012.05.037.

[26] Seyitoglu S, Dincer I, Kilicarslan A. Energy and exergy analyses of hydrogen production by coal gasification. Int J Hydrogen Energy 2017;42:2592–600. https://doi.org/10.1016/j.ijhydene.2016.08.228.

[27] Kida E, Ueda A, Takagi M, Koyama S. Entrained flow coal gasification development for a HYCOL pilot plant. Hitachi Rev 1995;44:19–24 [No longer findable on the internet].

[28] Osaki CoolGen Corporation. Overview of the Osaki CoolGen project. https://www.osaki-coolgen.jp/en/project/overview.html. [Accessed 8 December 2022].

[29] Field RP, Brasington R. Baseline flowsheet model for IGCC with carbon capture. Ind Eng Chem Res 2011;50:11306–12. https://doi.org/10.1021/ie200288u.

[30] Haslback J, Kuehn N, Lewis E, Pinkerton LL, Simpson J, Turner MJ, et al. Cost and performance baseline for fossil energy plants. Bituminous coal and natural gas to electricity, revision 2a. Pittsburgh, PA, Morgantown, WV: National Energy Technology Laboratory (NETL); 2013. https://www.osti.gov/biblio/1513268. [Accessed 8 December 2022].

[31] Based on confidential data provided by AGL Loy Yang power station.

[32] Australian Government. National Inventory Report. 2020. Volume 1, https://www.industry.gov.au/data-and-publications/national-greenhouse-accounts-2020/national-inventory-report-2020. [Accessed 8 December 2022].

[33] Thakur P, Graham-Bryce I, Karis W, Sullivan K. Global methane emissions from the world coal industry. Environ Monit Assess 1994;31:73—91. https://doi.org/10.1007/BF00547183.

[34] Kholod N, Evans M, Pilcher RC, Roshchanka V, Ruiz F, Coté M, et al. Global methane emissions from coal mining to continue growing even with declining coal production. J Clean Prod 2020;256:120489. https://doi.org/10.1016/j.jclepro.2020.120489.

[35] Tanner J, Kabir KB, Müller M, Bhattacharya S. Low temperature entrained flow pyrolysis and gasification of a Victorian brown coal. Fuel 2015;154:107—13. https://doi.org/10.1016/j.fuel.2015.03.069.

[36] Klutz H. Development status of WTA fluidized-bed drying for lignite at RWE Power AG. Power Plant Technology: Secure And Sustainable Energy Supply 2010;2:1—18. https://www.yumpu.com/en/document/view/11461709/development-status-of-wta-fluidized-bed-drying-for-rwecom. [Accessed 8 December 2022].

[37] Sayeed I, Kibria M, Bhattacharya S. Process modelling and techno-economic analysis of a 550MWe chemical looping power plant with victorian brown coal. Int J Greenh Gas Control 2022;113:103547. https://doi.org/10.1016/j.ijggc.2021.103547.

[38] Allardice D, Evans D. The-brown coal/water system: Part 2. Water sorption isotherms on bed-moist Yallourn brown coal. Fuel 1971;50:236—53. https://doi.org/10.1016/0016-2361(71)90014-7.

[39] Nagasaki N, Sasaki K, Suzuki T, Dodo S, Nagaremori F. Near-zero-emission IGCC power plant technology. Hitachi Rev 2013;62:39—47. 2013, https://www.hitachi.com/rev/pdf/2013/r2013_01_105.pdf. [Accessed 8 December 2022].

[40] Xu T, Bhattacharya S. Direct and two-step gasification behaviour of Victorian brown coals in an entrained flow reactor. Energy Convers Manag 2019;195:1044—55. https://doi.org/10.1016/j.enconman.2019.05.092.

[41] Aspen technology. Aspen plus model for entrained flow coal gasifier. https://user.eng.umd.edu/~nsw/chbe446/Aspen_Plus_Model_for_Entrained_Flow_Coal_Gasifier.pdf. [Accessed 8 December 2022].

[42] Kibria M, Sripada P, Woo M, Bhattacharya S. Fate of a biomass particle during CO_2 gasification: a mathematical model under entrained flow condition at high temperature. Energy 2019;168:1045—62. https://doi.org/10.1016/j.energy.2018.11.155.

[43] Tanner J, Bhattacharya S, Bläsing M, Müller M. High-temperature pyrolysis and CO_2 gasification of Victorian brown coal and Rhenish lignite in an entrained flow reactor. AIChE J 2016;62(6):2101—11. https://doi.org/10.1002/aic.15198.

[44] Billen P, Mazzotti M, Pandelaers L, Zhao W, Liu Z, Redus J, et al. Melt ceramics from coal ash: constitutive product design using thermal and flow properties. Resour Conserv Recycl 2018;132:168—77. https://doi.org/10.1016/j.resconrec.2018.01.035.

[45] Luberti M, Ahn H. Review of Polybed pressure swing adsorption for hydrogen purification. Int J Hydrogen Energy 2022;47(20):10911—33. https://doi.org/10.1016/j.ijhydene.2022.01.147.

[46] Lee D-Y, Elgowainy A. By-product hydrogen from steam cracking of natural gas liquids (NGLs): potential for large-scale hydrogen fuel production, life-cycle air emissions reduction, and economic benefit. Int J Hydrogen Energy 2018;43:20143—60. https://doi.org/10.1016/j.ijhydene.2018.09.039.

[47] Cardella U, Decker L, Klein H. Final design of a cost-optimized 100 tpd H_2 liquefier. Cryogenic engineering conference and international cryogenic materials conference 2017;1:1—14. https://indico.cern.ch/event/763185/contributions/3167011/attachments/1727919/2791769/C3OrJ__2017.pdf. [Accessed 8 December 2022].

[48] Aspen Technology. Rate-based model of the CO_2 capture process by MDEA using aspen plus. 2016. https://pdfcoffee.com/enrtl-rk-rate-based-mdea-model-pdf-free.html. [Accessed 8 December 2022].

[49] Manouchehrinejad M, van Giesen I, Mani S. Grindability of torrefied wood chips and wood pellets. Fuel Process Technol 2018;182:45—55. https://doi.org/10.1016/j.fuproc.2018.10.015.

[50] Güngör A, Önenç S, Uçar S, Yanik J. Comparison between the "one-step" and "two-step" catalytic pyrolysis of pine bark. J Anal Appl Pyrol 2012;97:39—48. https://doi.org/10.1016/j.jaap.2012.06.011.

[51] Mohan D, Pittman Jr CU, Bricka M, Smith F, Yancey B, Mohammad J, et al. Sorption of arsenic, cadmium, and lead by chars produced from fast pyrolysis of wood and bark during bio-oil production. J Colloid Interface Sci 2007;310(1):57—73. https://doi.org/10.1016/j.jcis.2007.01.020.